Transition Behavior of Block Copolymer Thin Films on Preferential Surfaces

Changhak Shin,[†] Hyungju Ahn,[†] Eunhye Kim,[†] Du Yeol Ryu,*[,†] June Huh,[†] Kwang-Woo Kim,[‡] and Thomas P. Russell*[,§]

Department of Chemical Engineering and Active Polymer Center for Pattern Integration, Yonsei University, Seoul 120-749, Korea, Pohang Accelerator Laboratory, Pohang 790-784, Korea, and Department of Polymer Science & Engineering, University of Massachusetts, Amherst, Massachusetts 01003

Received August 5, 2008; Revised Manuscript Received September 21, 2008

ABSTRACT: The phase transitions in block copolymers (BCPs), like the order-to-disorder transition, occur when the enthalpic term of free energy of mixing is equal to the entropic term. In thin films, interactions at the substrate/polymer and polymer/air interfaces influence this free energy balance, leading to a change in the transition behavior. Here, we report on the transition behavior of BCP thin films on a substrate modified by polymer chains that preferentially interact with one component of the BCP. The thickness dependence of the transition temperature shows that interfacial interactions enhance the orientation of the lamellar microdomain parallel to the film surface even in 40 L_0 in thickness, where L_0 is the equilibrium period of the BCP in the bulk. This phenomenon can be attributed to the fact that, in a thin film geometry with a preferential interaction of one component with the substrate, a high concentration of one component is pinned at the substrate leading to an amplification of a periodic variation in the composition and a shift of transition temperature.

Introduction

Block copolymers (BCPs) have received significant attention recently as templates and scaffolds for the fabrication of nanostructured materials,[1,2] for example, in pattern lithography,[3] templates for storage devices,[4] optical materials,[5] nanowires,[6] and membranes.[7] BCPs consisting of chemically different polymers covalently linked together at one end can self-assemble in tens of nanometers into ordered arrays lamellar, cylindrical, gyroid, and spherical microdomains depending on the volume fraction of the blocks. In the bulk, the microphase separation occurs provided the product χN is sufficiently large ($\chi N \gg 10.5$ in the case of symmetric BCPs), where χ is the segmental interaction parameter and N is the total number of segments in the BCP.[8−10] When χ is inversely proportional to temperature (T), BCPs are phase-mixed at elevated temperature and microphase-separate upon cooling. The transition from the ordered to the disorder state occurs at a temperature of T_{ODT}, where the nonfavorable segmental interactions are sufficiently weakened and entropy dominates.[11] Several techniques have been used to determine this transition due to the changes in the enthalpy, rheology, optical properties, and morphology, including differential scanning calorimetry (DSC),[12] rheological measurements,[13] birefringence,[14] small-angle X-ray scattering (SAXS), and small-angle neutron scattering (SANS).[15]

In thin films, the behavior of BCPs differs appreciably from the bulk due to the interfacial interactions.[16,17] The phase transition of BCP thin films on Si substrates was first evaluated by ex-situ neutron reflectivity (NR), leading to the thickness dependence on T_∞, at which the decay length (ξ) reduces discontinuously with increasing temperature.[18] Unlike a T_{ODT}, this transition temperature was defined as the order to a partially disordered transition since the order parameter, characterized by concentration or scattering length density, never achieved a constant value equal to the average value of the copolymer. For thick films ($\gg\xi$) even well-above T_{ODT}, strong periodic variations in the concentrations of the components normal to the interface are seen due to the pinning of a high concentration of one component at the interface, while the middle of the film still is disordered.[19] Technically though, ξ approaches infinity at the T_{ODT}, but the random nucleation of microphase separation at distances far from the interface prohibits the propagation of order through the entire film.

Near the substrate interface, an orientation of the microdomains parallel to the plane of the interface occurs when there is a preferential interaction of one block with the substrate. This orientation propagates into the films by an amount that is dictated by the strength of the interfacial interactions.[20] For ultrathin BCP films, the interfacial interactions can also influence the phase behavior of BCP because the interactions are more effective and then enough to alter the phase behavior of thin films, although the transition behavior in thin films of BCPs is not well-defined.

In this study, the order-to-disorder transition for lamella-forming PS-*b*-PI (hereafter denoted as SI) was investigated by in situ grazing incidence small-angle X-ray scattering (GISAXS) as a function of the film thickness ranging 2 L_0 to thick 40 L_0 in order to assess thickness dependence on the transition temperature and compare with the bulk phase behavior measured.

Experimental Section

A symmetric BCP composed of polystyrene and polyisoprene, denoted as SI-23K, was synthesized by the sequential anionic polymerization of styrene and isoprene in cyclohexane at 45 °C under purified argon using *sec*-butyllithium as an initiator. Molecular weight (M_n) and polydispersity index (PDI), characterized by size-exclusion chromatography (SEC) with the multiangle laser light scattering (MALLS), were 23 000 and 1.04, respectively. PS volume fraction (Φ_{PS}) of BCP was determined to be 0.46 by ^{1}H nuclear magnetic resonance (^{1}H NMR) with mass densities of two components (1.05 and 0.90 g/cm^3 for PS and PI). An hydroxyl-terminated polystyrene (PS-OH) was synthesized via anionic polymerization (Polymer Source), having $M_n = 10\,000$ and PDI = 1.09, to prepare a selectively preferential PS brush.

* To whom correspondence should be addressed. E-mail dyryu@yonsei.ac.kr (D.Y.R.) and russell@mail.pse.umass.edu (T.P.R).
[†] Yonsei University.
[‡] Pohang Accelerator Laboratory.
[§] University of Massachusetts.

10.1021/ma801778m CCC: $40.75
Published on Web 11/06/2008

PS was anchored to the Si substrate by spin coating a thin film of PS-OH from toluene then annealing at 170 °C under vacuum for 3 days. During annealing well-above the glass transition temperatures (T_g) of PS (<100 °C), end-functional hydroxyl groups of PS-OH diffuse to and react with the native oxide layer, hence producing a PS brush to the substrate. After rinsing with toluene to remove the nonanchored chains, the thickness of PS brush was measured to be 5.0 ± 0.3 nm by ellipsometry (SE MG-1000, Nanoview Co.). BCP films, having thicknesses ranging from 35 nm (2 L_0) to 685 nm (40 L_0), were spin coated from toluene solution onto the bare Si substrates and the PS-modified substrate. Subsequently, the thin films were annealed at 100 °C under vacuum for 24 h to allow the chain mobility sufficiently between T_g and T_{ODT}.

X-ray scattering experiments were carried out at 4C1 (SAXS) and 4C2 (GISAXS) beam-lines at the Pohang Accelerator Laboratory (PAL), Korea. The operating conditions were set to a wavelength of 1.54 Å and the sample-to-detector distance of 2.5 m. The samples were mounted on a heating cell under vacuum, and the incident angle was set at 0.16 ° or 0.18 °, which are above the critical angle (0.15°) of BCP thin films. [19] Two-dimensional (2D) GISAXS patterns were recorded using a CCD detector (Princeton Instruments) positioned at the end of a vacuum guide tube when the X-ray beam passes through the BCP thin films under vacuum (5×10^{-4} torr). Small-angle X-ray scattering (SAXS; 4C1 beamline) was used to determine the bulk behavior of the BCP. All of the heating experiments were controlled automatically with a PID temperature controller from 40 to 160 °C at constant heating rate 0.9 °C/min and with the exposure time of 120 s.

Result and Discussion

SAXS intensity profiles for bulk SI-23K, measured at various temperatures during heating at a heating rate of 0.9 °C/min from 70 to 160 °C, are shown in Figure 1a as a function of the scattering vector (q), where $q = (4\pi/\lambda) \sin\theta$ and 2θ and λ are the scattering angle and wavelength, respectively. At low temperatures (T < 100 °C), a sharp scattering peak and the higher-order peaks (indicated by arrow) located at integral values of q relative to the first order reflection are observed, characteristic of the lamellar microdomain morphology. With increasing temperature (T > 122 °C), the primary peak weakens and broadens abruptly and the second-order reflection disappears, which is the classic correlation hole scattering of a phase-mixed BCP. Consequently, a T_{ODT} = 122 ± 1 °C can readily be determined for bulk SI-23K from the discontinuous changes of the scattering parameters derived from the SAXS profiles, like the inverse of the maximum intensity ($1/I(q_{max})$), full width at half-maximum (fwhm), and domain spacing (d) by $d = 2\pi/q_{max}$ as a function of inverse temperature (1/K), as plotted in Figure 1b. This behavior is typical for BCPs undergoing a transition from the ordered to disordered state.

2D GISAXS patterns for SI-23K film with thickness of 431 nm on the PS-modified substrate are shown in Figure 2 after thermally annealing at 100 °C for 24 h. This thickness corresponds to ~25 L_0, where L_0 is the domain spacing ($d = 2\pi/q_{max}$) of 17.0 nm, taken at a temperature of 80 °C. All patterns were obtained during heating thin film from 80 to 160 °C at a heating rate of 0.9 °C/min, followed by cooling to 100 °C. In the scattering geometry used, q_y is the scattering vector normal to the incident plane, and q_z is the scattering vector normal to the sample surface, defined as $q_z = (4\pi/\lambda) \sin\theta$. The d spacing is related to q_y by $d = 2\pi/q_y$. The incidence angle was set at 0.18° (greater than the critical angle of the BCP) to probe the morphology of the entire film.

For T = 80 °C, the GISAXS pattern does not show any in-plane scattering peak at $q_y = 0.370$ nm^{-1} ($2\pi/d$) but, rather, shows two distinct specular scattering peaks along q_z near $q_y = 0$, as shown in Figure 2. This arises from the correlated roughness at interfaces for the multilayered lamellar microdomains aligned parallel to the film surface.[21,22] The parallel orientation of the lamellar microdomains is evident in the thin film even at 129 °C which is higher than the T_{ODT} of bulk SI-23K. With further increasing temperature, the in-plane scattering peaks along q_y at constant $q_z = 0.287$ nm^{-1} (corresponding to q_z of the reflected beam) begin to appear at 131 °C, intensify, and reach the consistent maxima up to 160 °C. Two distinct specular peaks along q_z near $q_y = 0$ (along the vertical beamstop), however, decrease in intensity with increasing temperature. In addition to these changes, two elliptical scattering patterns are observed for T > 135 °C, which arise from the correlation hole scattering from a disordered BCP in the thin film. The ellipticity of the scattering patterns indicates that even in the disordered state the interfaces are biasing the fluctuations in the thin film. Upon cooling to 100 °C, the in-plane scattering peaks disappear and the scattering peaks along q_z (near $q_y = 0$) reappear although there is minor hysteresis, as can be seen for the thin film at 130 °C in Figure 2. These results confirm the thermo-reversibility for this transition.

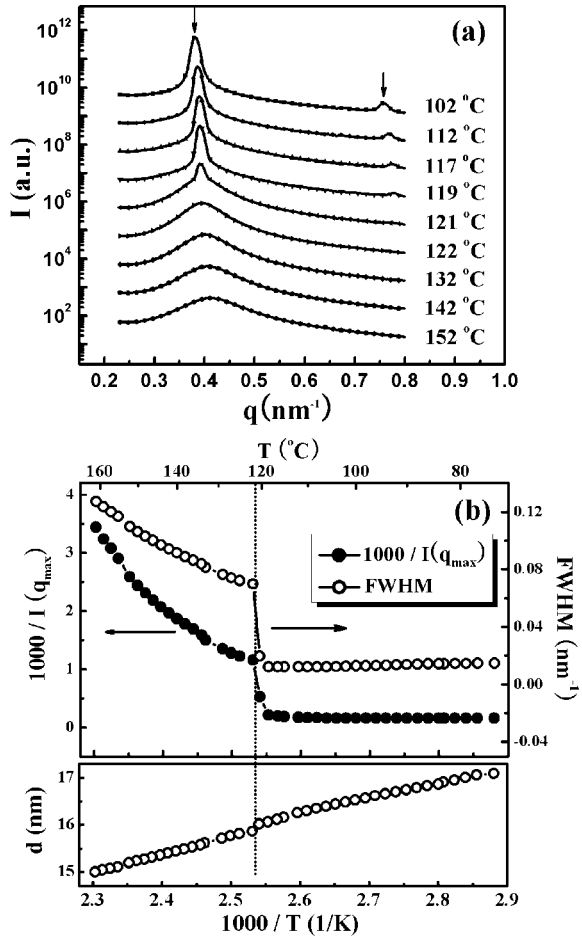

Figure 1. (a) SAXS intensity for bulk SI-23K as a function of scattering vector (q) at various temperatures ranging from 70 to 160 °C at a heating rate of 0.9 °C/min, and (b) the scattering parameters derived from SAXS profiles. The inverse of the maximum intensity ($1/I(q_{max})$), full width at half-maximum (fwhm), and domain spacing by $d = 2\pi/q_{max}$ are plotted as a function of inverse temperature (1/K).

GISAXS patterns for thin films of lamella-forming BCP have been analyzed using the distorted-wave Born approximation (DWBA),[21] enabling an analytic calculation of the scattering profiles in q_z at $q_y = 0$ for lamellar microdomains oriented parallel to the film surface, by

$$q_z = \frac{2\pi}{\lambda}\left(\pm\sin\alpha_i + \sqrt{\sin^2\alpha_{cP} + \left[\frac{m\lambda}{L_0} \pm \sqrt{\sin^2\alpha_i - \sin^2\alpha_{cP}}\right]^2}\right) \quad (1)$$

This assumes that the thin film is homogeneous across the substrate with alternating lamellar layers composed of PS and PI, which can be treated as a perturbation.[21] Where α_i and α_{cp} are the incident (0.18°) and critical angles (0.15°), respectively, and m is a positive, odd integer for the symmetric lamellar structure. From this simple calculation for the film of 25 L_0, scattering peaks at two q_z were obtained at 0.44 and 0.62 nm^{-1} ($\alpha_i = 0.18°$ and $m = 1$), which are in good agreement with the experimental results, as indicated by the arrows in Figure 2 and 3a. These corresponding peaks represent a multilayered lamellar microdomain structure aligned parallel to the film surface at lower temperatures.

For better statistics, the intensity profiles from the GISAXS patterns in Figure 2 are scanned along q_y direction at constant

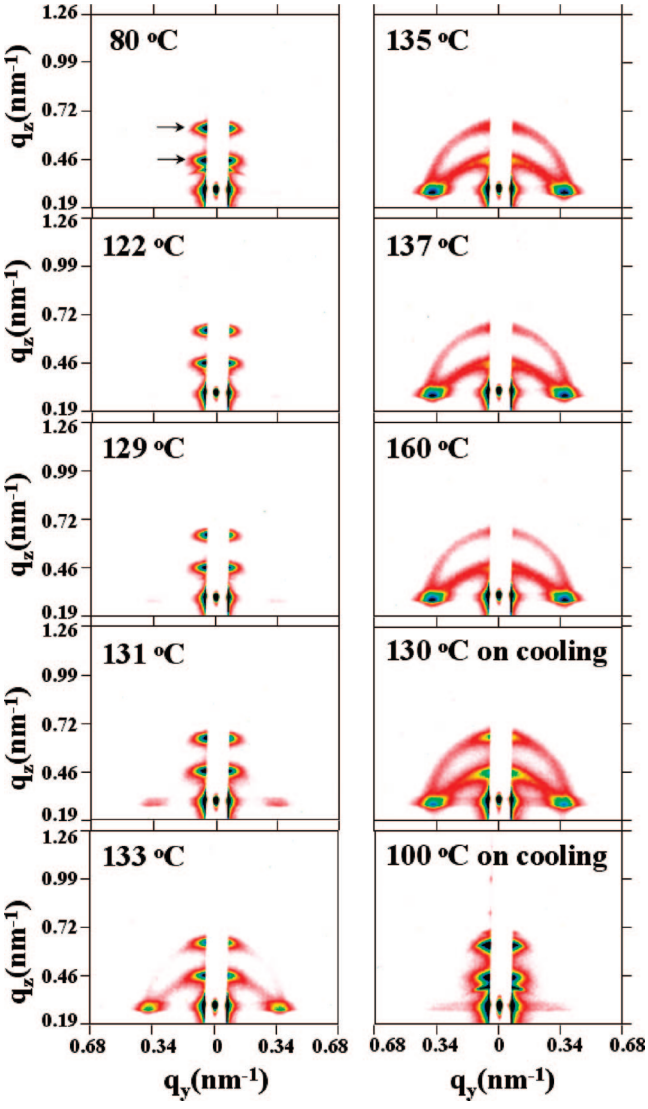

Figure 2. 2D GISAXS patterns for SI-23K film with thickness of 431 nm (25 L_0) on the PS-modified substrate at incident angle of 0.18°, which is above the critical angles for SI copolymer (0.15°) and SiO_2 (0.22°). All patterns were taken during heating at a heating rate of 0.9 °C/min and then cooling to 100 °C after thermally annealing at 100 °C under vacuum for 24 h. Arrows indicate two peak positions of the specular scattering at $q_z = 0.44$ and 0.62 nm^{-1} ($\alpha_i = 0.18°$ and $m = 1$) from the simple calculation by eq 1, which corresponds to two arrows in Figure 3.

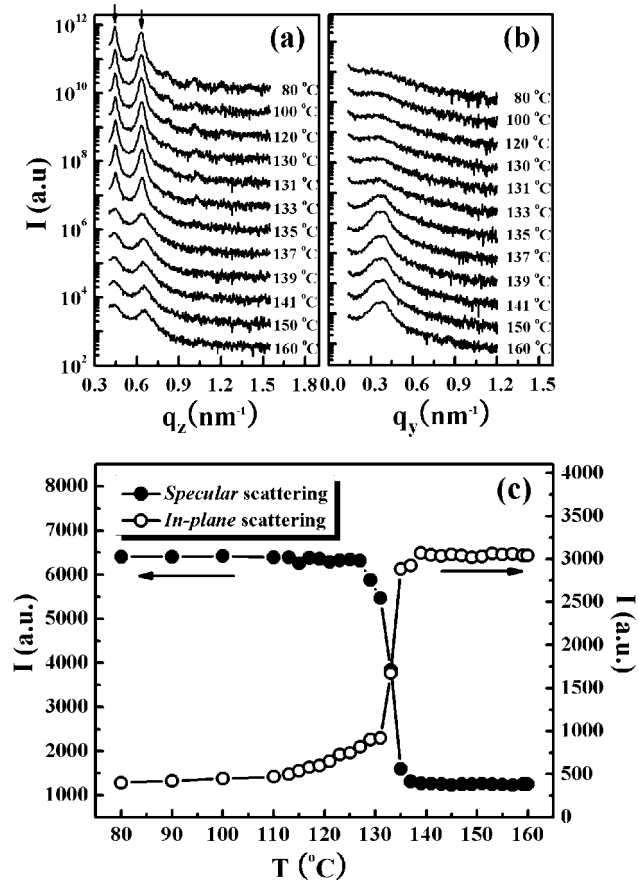

Figure 3. Intensity profiles from GISAXS patterns in Figure 2 for SI-23K film with thickness of 25 L_0 at both (a) the specular scattering scanned along q_z direction near $q_y = 0$ during heating thin film and (b) the in-plane scattering scanned along q_y direction at constant $q_z = 0.287$ nm^{-1} (corresponding to q_z of the reflected beam), respectively. (c) the maximum intensities of both peaks as a function of temperature. By the clear discontinuity at 135 °C, the multilayered lamellar microdomains become to disordered state in thin film at greater than 135 °C. Interestingly, the same transition temperatures were observed for SI-23K films with thicknesses of 40 L_0 and 12 L_0 on the PS-modified substrate.

$q_z = 0.287$ nm^{-1} and along q_z direction near the vertical beamstop ($q_y = 0$), as shown in Figure 3a,b, respectively. These results support the structural changes of the entire film of 25 L_0 during heating. It is worthwhile to note that the scattering peaks along q_z for $T = 80$ to 133 °C are even sharper than the in-plane scattering peaks along q_y in the disordered state at higher temperatures from $T = 137$ to 160 °C. The temperature dependences of both peak intensities in Figure 3c exhibit a distinct discontinuity at 135 °C, indicative of the order-to-disorder transition. The identical transition temperature was observed for SI-23K films with thicknesses of 205 nm (12 L_0) and 685 nm (40 L_0) on the PS-modified substrate, which is still higher than the T_{ODT} (122 °C) of bulk SI-23K. This can be attributed to the pinned high concentration of one component at the substrate, leading to the suppression of fluctuations and a perfect multilayered lamellar microdomain parallel to the film surface, as evidenced by the TEM image for SI-23K film with thickness of 40 L_0 in Figure 4.

Neutron reflectivity (NR) results of Menelle et al.[18] indicate that the transition in the thin films, unlike that in the bulk, is one where the BCP changes from being in the ordered state to a partially disordered state, since, even at elevated temperatures, the order parameter never reaches a constant value equal to the average composition of the BCP. Interfacial interactions cause a pinning of a high concentration of one component that leads

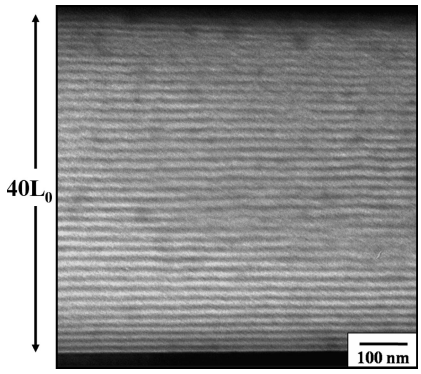

Figure 4. TEM image for SI-23K film with thickness of 40 L_0 on the PS-modified substrate, which was taken by quenching from 100 °C. Polyisoprene block was selectively stained with OsO_4 to increase the contrast.

to a damped oscillatory variation in the composition propagating into the film. However, the discontinuous changes of intensity observed in this study is quite similar to that seen in the bulk and within the interior of the films, and a truly disordered state was attained. The origin of the differences in these two studies is, more than likely, the temperature dependence of χ between polystyrene-*block*-poly(methyl methacrylate) (PS-*b*-PMMA) and SI, where the temperature dependence of χ is quite small, almost independent of temperature for PS-*b*-PMMA, whereas for SI, the temperature dependence of χ is quite strong, forcing the BCP more deeply into the disordered state, or conversely, significantly decreasing the decay length.

2D GISAXS patterns for SI-23K films with thickness of 103 nm (6 L_0) on the PS-modified substrate are shown in Figure 5a. All patterns were obtained during heating from 80 to 160 °C, followed by cooling to 100 °C. For T < 135 °C, two specular scattering peaks (indicated by arrows from eq 1) are evident along q_z near $q_y = 0$ due to the multilayered lamellar microdomains oriented parallel to the film surface, although the peak intensities are weaker in comparison to those seen for the film of 25 L_0 by the thickness difference. With increasing temperature, the in-plane scattering peaks along q_y at constant $q_z = 0.287$ nm^{-1} as well as two elliptical scattering patterns appear at $T = 147$ °C and remain this way up to 160 °C. These results indicate a thermo-reversible transition temperature between 135 and 147 °C. However, the GISAXS patterns for the film of 68 nm (4 L_0) did not show the elliptical scattering patterns, more than likely because of the thin film thickness. It should be noted that the thinner the films, the more stretched are the in-plane scattering patterns along q_y due to a waveguide resonances by the correlated interferences of the film.[23]

For the very thin film (35 nm or 2 L_0) of SI-23K on the PS-modified substrate, 2D GISAXS patterns are given in Figure 5b for each temperature. The scattering peaks along q_z near $q_y = 0$ are very weak and the intensities of in-plane scattering peaks appear along q_y at constant $q_z = 0.254$ nm^{-1}, while weak at $T \sim 120$ °C, then gradually increase in intensity for $T =$ 139.5 to 160 °C with no discernible transition. Upon cooling to 100 °C, the intensity decreases. This thermo-reversible phenomenon corresponds to the fact that at higher temperature the ordered microdomain layers remain at the interfaces for a very thin film of 2 L_0 although the scattering intensities change in accordance with the degree of phase segregation, resulting from the effective interfacial interactions by the PS-modified substrate, as will be discussed later.

In contrast, Figure 6 shows the maximum intensities of specular and in-plane scattering from GISAXS patterns for SI-23K film with thickness of 25 L_0 on the bare Si substrate. The temperature dependences of both peak intensities exhibit a clear

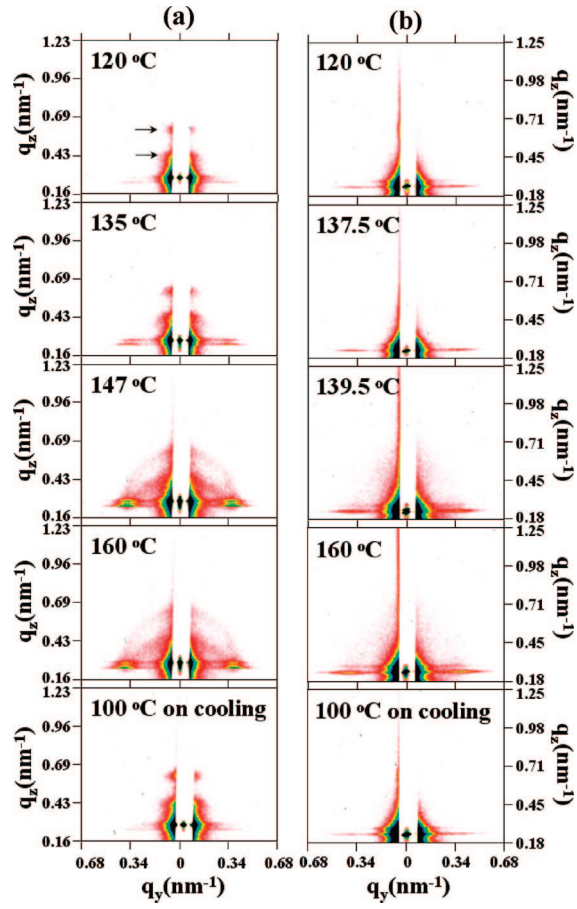

Figure 5. 2D GISAXS patterns for SI-23K films with (a) thickness of 103 nm (6 L_0) at incident angle of 0.18° and (b) thickness of 35 nm (2 L_0) at incident angle of 0.16° on the PS-modified substrate. All patterns were taken during heating process at a heating rate of 0.9 °C/min and then cooling to 100 °C after thermally annealing at 100 °C under vacuum for 24 h. Arrows indicate two peak positions of specular scattering at $q_z = 0.44$ and 0.62 nm^{-1} ($\alpha_i = 0.18°$ and $m = 1$) from the simple calculation by eq 1.

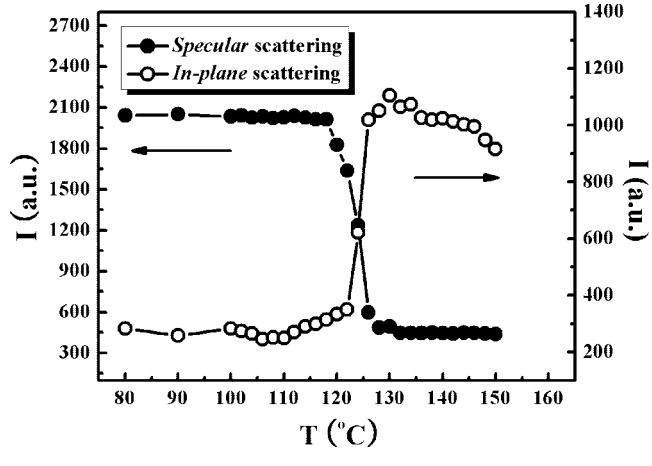

Figure 6. The maximum intensities of specular and in-plane scattering from GISAXS patterns for SI-23K film with thickness of 25 L_0 on the bare Si substrate during heating thin film. The specular and in-plane scattering were scanned along q_z direction near $q_y = 0$, and along q_y direction at constant $q_z = 0.287$ nm^{-1} (corresponding to q_z of the reflected beam), respectively. By the clear discontinuity at 123 °C the lamellar microdomains become to disordered state in thin film.

discontinuity at 123 °C which is similar to that for bulk SI-23K, indicating that the lamellar microdomains of SI-23K on the bare Si substrate come to a disordered state in thin film.

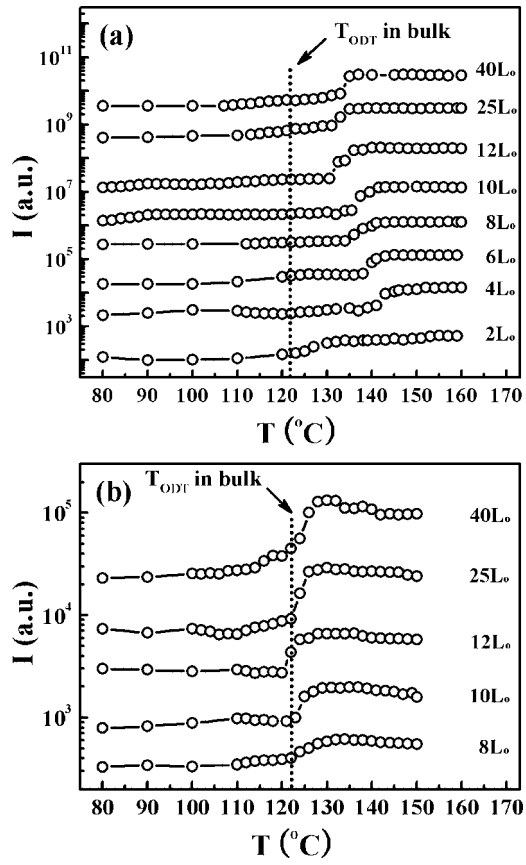

Figure 7. The maximum intensities of in-plane scattering, scanned along q_y direction at constant q_z, as a function of temperature for SI-23K films (a) on the PS-modified substrate and (b) on the bare Si substrate during heating at a heating rate of 0.9 °C/min. The dotted line guides T_{ODT} (122 °C) for bulk SI-23K.

Different from the thin film geometry with a preferential interaction of one component with the substrate such as the PS-modified substrate, weak interactions at the oxide/polymer interfaces little influence the free energy balance, leading to a consistency in the transition temperatures as are the cases for SI-23K films with thicknesses of 209 nm (12 L_0) and 695 nm (40 L_0) on the bare Si substrate.

An intensity of the maximum in the in-plane scattering peak was plotted as a function of temperature at constant $q_z = 0.254$ nm^{-1} for SI-23K films of 2 L_0 and 4 L_0, and at constant $q_z = 0.287$ nm^{-1} for the other thicknesses, up to 40 L_0 in Figure 7 depending on the substrates. For the film of 40 L_0 on the PS-modified substrate as shown in Figure 7a, the low intensity of in-plane scattering peak by the multilayered lamellar microdomains aligned parallel to the film surface increases rapidly at 135 °C because of the correlation hole scattering from a disordered state for the thin BCP film. These transition temperatures at 135 °C, as confirmed by the discontinuous change of intensity, are the same as those for the films of 25 L_0 and 12 L_0, whereas for bulk SI-23K, $T_{ODT} = 122$ °C (guided by dotted line) which is significantly lower than that seen in these thin films. As the film thickness decreases from 10 L_0 to 4 L_0, the transition temperatures increase to 147 °C. A very thin film of 2 L_0 thickness does not show any discernible transition. However, the intensity gradually increases up to 160 °C, confirming the ordered state of lamellar microdomains over the experimentally accessible temperature range as described in Figure 5b. However, for the films of 12 L_0, 25 L_0, and 40 L_0 on the bare Si substrate in Figure 7b, the low intensity of in-plane scattering peak also increases rapidly at 123 °C which is nearly identical to that (122 °C) for bulk SI-23K within

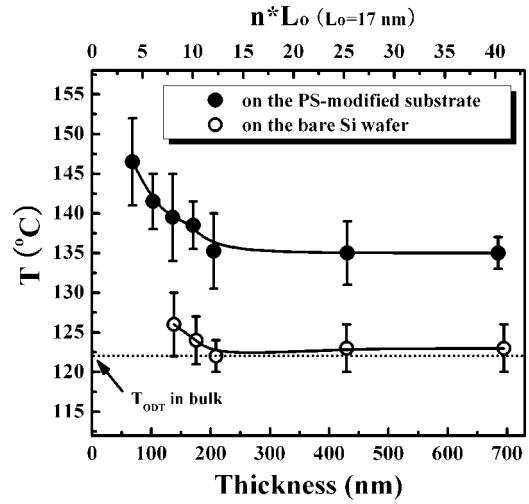

Figure 8. Transition temperatures as a function of film thickness for SI-23K films on the PS-modified substrate and the bare Si substrate. These transition temperatures by the discontinuous change of intensity were determined in the middle points of temperature range. Error bars indicate the initial and final points of transition temperatures and the dotted line guides T_{ODT} (122 °C) for bulk SI-23K.

experimental error range of ±1 °C possibly due to the change from the random orientation of lamellar microdomain to a disordered state for the thin BCP film. As the film thickness decreases from 10 L_0 to 8 L_0, the transition temperatures discernible by the discontinuous change of intensity increase to 126 °C with a broad range. Unfortunately, no discernible transition is seen for SI-23K films thinner than 8 L_0.

A summary of the thickness dependence of transition temperature is shown in Figure 8. First, for the films with thicknesses less than 12 L_0 on the PS-modified substrate, T_{ODT} increases with decreasing thickness, while a little increase is seen in thin films on the bare Si substrate. This ultimately leads to the ordered state of lamellar microdomains for the ultrathin film where no disordering transition is seen for thin film of 2 L_0 on the PS-modified substrate. This thickness dependence of the transition temperature on the substrates can be attributed to the fact that in a thin film geometry with a preferential interaction of one component with the substrate, the strength of interfacial interactions inversely proportional to the film thickness as would be expected. The second is that, for SI-23K films with thicknesses greater than 12 L_0 on the PS-modified substrate, T_{ODT} (135 °C) is significantly shifted from the bulk T_{ODT} (122 °C) by 13 °C. This difference, again, can be attributed to the strength of the interactions between the PS-modified substrate and PS block of SI-23K and the extent to which the ordering and orientation of the lamellar microdomain morphology propagates into the film. Therefore, the surface effect of the transition temperature shows that the preferential interactions with one component of the BCP can lead to a shift of transition temperature, as a consequence of an amplification of a periodic variation in the composition and the enhanced orientation of the lamellar microdomain parallel to the film surface even for the film of 40 L_0. In support of this, in the thin films where the interfacial interactions are weakened, as is the case for a bare Si substrate, the T_{ODT} of films (25 L_0) were nearly equal to that seen in the bulk SI-23K.

Acknowledgment. This work was supported by the Korea Research Foundation Grant (KRF-2007- D00230), and APCPI ERC program (R11-2007-050-01004) funded by the Ministry of Education, Science & Technology (MEST), Korea, and T.P.R. acknowledges the support of the Department of Energy, Office of Basic Energy Sciences.

References and Notes

(1) Hamley, I. W. *The Physics of block copoymers*, Oxford University Press, New York, 1998.
(2) Ruzette, A.-V.; Leibler, L. *Nat. Mater.* **2005**, *27*, 19–31.
(3) Park, M.; Harrison, C.; Chaikin, P. M.; Register, R. A.; Adamson, D. H. *Science* **1997**, *276*, 1401–1404.
(4) Fasolka, M. J.; Mayes, A. M. *Ann. Rev. Mater. Res.* **2001**, *31*, 323–355.
(5) Kang, Y.; Walish, J. J.; Gorishnyy, T.; Thomas, E. L. *Nat. Mater.* **2007**, *6*, 957–960.
(6) Black, C. T. *Nat. Nano.* **2007**, *2*, 464–465.
(7) Lazzari, M.; Lopez-Quintela, M. A. *Adv. Mater.* **2003**, *15*, 1583–1594.
(8) Hashimoto, T. *Thermoplastic Elastomers,* Hanser: New York, 1987.
(9) Bates, F. S.; Fredrickson, G. H. *Annu. Rev. Phys. Chem.* **1990**, *41*, 525–557.
(10) Leibler, L. *Macromolecules* **1980**, *13*, 1602–1617.
(11) Almdal, K.; Rosedale, J. H.; Bates, F. S.; Wignall, G. D.; Fredrickson, G. H. *Phys. Rev. Lett.* **1990**, *65*, 1112–1115.
(12) Voronov, V. P.; Buleiko, V. M.; Podneks, V. E.; Hamley, I. W.; Fairclough, J. P. A.; Ryan, A. J.; Mai, S.-M.; Liao, B.-X.; Booth, C. *Macromolecules* **1997**, *30*, 6674–6676.
(13) Rosedale, J. H.; Bates, F. S. *Macromolecules* **1990**, *23*, 2329–2338.
(14) Wang, H.; Newstein, M. C.; Chang, M. Y.; Balsara, N. P.; Garetz, B. *Macromolecules* **2000**, *33*, 3719–3730.
(15) Bates, F. S.; Rosedale, J. H.; Fredrickson, G. H. *J. Chem. Phys.* **1990**, *92*, 6255–6270.
(16) Green, P. F.; Limary, R. *Adv. Colloid Interface Sci.* **2001**, *94*, 53–81.
(17) Riegler, H.; Kohler, R. *Nat. Phys.* **2007**, *3*, 890–894.
(18) Menelle, A.; Russell, T. P.; Anastasiadis, S. H.; Satija, S. K.; Majkrzak, C. F. *Phys. Rev. Lett.* **1992**, *68*, 67–70.
(19) Milner, S. T.; Morce, D. C. *Phys. Rev. E* **1996**, *54*, 3793–3810.
(20) Russell, T. P.; Coulon, G.; Deline, V. R.; Miller, D. C. *Macromolecules* **1989**, *22*, 4600–4606.
(21) Busch, P.; Rauscher, M.; Smilgies, D. M.; Posselt, D.; Papadakis, C. M. *J. Appl. Crystallogr.* **2006**, *39*, 433–442.
(22) Busch, P.; Posselt, D.; Smilgies, D. M.; Rauscher, M.; Papadakis, C. M. *Macromolecules* **2007**, *40*, 630–640.
(23) Narayanan, S.; Lee, D. R.; Guico, R. S.; Sinha, S. K.; Wang, J. *Phys. Rev. Lett.* **2005**, *94*, 145504–145504.

MA801778M